V.I. ABROSIMOV, O.I. DAVYDOVSKA

Institute for Nuclear Research, Nat. Acad. Sci. of Ukraine
(47, Prospect Nauky, Kyiv 03680, Ukraine; e-mail: abrosim@kinr.kiev.ua)

# NATURE OF ISOSCALAR DIPOLE RESONANCES IN HEAVY NUCLEI

The isoscalar dipole nuclear response reveals low- and high-energy resonances. The nature of isoscalar dipole resonances in heavy spherical nuclei is studied, by using a translation-invariant kinetic model of small oscillations of finite Fermi systems. Calculations of the velocity field at the centroid energy show a pure vortex character of the low-energy isoscalar dipole resonance in spherical nuclei and confirm the anisotropic compression character of the high-energy one. The evolution of the velocity field as a function of the excitation energy of the nucleus within the resonance width is studied. It is found that the low-energy isoscalar dipole resonance retains a vortex character, while with this collective excitation also involves a compression, as the energy increases. The high-energy resonance keeps the compression character with a change in the excitation energy within the resonance width, but the compression-expansion region of the velocity field related to this resonance shifts inside the nucleus.

K e y w o r d s: kinetic model, isoscalar dipole nuclear response, velocity field, vortex and compression modes.

1. Introduction

Recent experiments have shown that the isoscalar dipole nuclear response reveals not only the compression dipole mode (the high-energy resonance), but also a low-energy resonance [1–4]. Theoretical studies of the nuclear isoscalar dipole excitations had been carried out within quantum approaches [5–11], as well as within semiclassical ones [12–16]. It was found that the low-energy isoscalar dipole resonance has an essentially vortex character [17–21]. It is of interest to further study the nature of this resonance. For this purpose, it is suitable to consider the velocity field related to the resonance. This local dynamic quantity describes the spatial distribution of the average nucleon velocity under a collective excitation and provides information on the nature of the excitation. In this paper, the collective isoscalar dipole excitations are considered within the translation-invariant kinetic model of small oscillations of finite Fermi systems [21]. The model is based on the collisionless kinetic equation in the mean-field approximation (the Vlasov kinetic equation). Our model makes it possible to find an analytic expression for the dynamic fluctuations of the distribution function in the phase space under collective isoscalar dipole excitations. By using this solution, one can obtain an explicit expression for the velocity field, which is a local quantity that depends on the excitation energy of the system. In Ref. [22], the isoscalar dipole response function was studied within the kinetic model [22] with regard for a residual interaction between nucleons that is related to the mean-field fluctuations. It was found that the response function has two-resonance structure and reproduces the experimental values for the centroid energies of the low- and high-energy isoscalar dipole resonances in heavy nuclei. We will use this response function in the present paper.
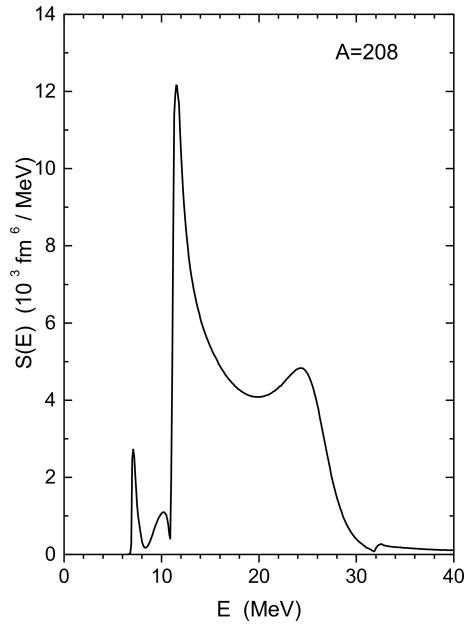
Fig. 1. Isoscalar dipole strength function for a system of $A = 208$ interacting nucleons [23]

In Section 2, the analytic expression of the velocity field related to the isoscalar dipole excitations is presented within the translation-invariant kinetic model of small oscillations of finite Fermi systems. To study the nature of the isoscalar dipole resonances in nuclei, the evolution of the velocity field character depending on the excitation energy of the nucleus within the resonance width is investigated (Section 3). In Appendix A, the explicit expression for the dynamic fluctuations of the phase-space distribution function under the collective isoscalar dipole excitations is derived.

2. Velocity Field in Kinetic Model

We consider the isoscalar dipole excitations of nuclei within a kinetic model, which is based on the Vlasov equation for finite Fermi systems with moving surface [15, 22, 23]. In this model, a nucleus is treated as a gas of interacting fermions confined to a spherical cavity with moving surface. We calculate the response of nuclei to a weak external field of the kind

$$V(\mathbf{r}, t) = \beta \delta(t)\, Q^{(3)}(r)\, Y_{10}(\theta, \varphi), \qquad (1)$$

where $Q^{(3)}(r) = r^3$ is the second-order dipole moment, $\delta(t)$ is the Dirac delta-function of the time, and β is a parameter that describes the external field strength. Our model is translation-invariant

[15, 23]. Therefore, the external field (1) does not excite the center of mass. We consider the residual interaction between nucleons, by using a separable effective interaction of the dipole-dipole type [23]. Within our kinetic model, we can find the explicit expression for the fluctuation of the phase-space distribution function related to the collective isoscalar dipole excitations. By using this function, we can calculate the response function [23] as well as the local dynamical quantities, in particular, the velocity field.

In our kinetic model, the time Fourier-transform of the velocity field in the linear approximation is determined as

$$\mathbf{u}(\mathbf{r}, \omega) = \frac{1}{m\rho_0} \int d\mathbf{p}\, \mathbf{p}\, \delta n(\mathbf{r}, \mathbf{p}, \omega), \qquad (2)$$

where $\mathbf{r}$, $\mathbf{p}$ are the radius-vector and momentum of the particle, respectively; ρ_0 is the nuclear matter density at equilibrium, and $\delta n(\mathbf{r}, \mathbf{p}, \omega)$ is a variation of the particle distribution function in the phase space, which is caused by the action of an external field (1). In Eq. (2), the value of ω defines the excitation energy of the nucleus ($E = \hbar\omega$).

Taking the Z-axis in the direction of the external field, we are interested in the velocity field in the meridian plane XZ ($\mathbf{r} = (x, y = 0, z)$ or in the spherical coordinates $\mathbf{r} = (r, \theta, \phi = 0)$) that are usually exploited in the RPA calculations [11, 24].

Then the velocity field can be written as

$$\mathbf{u}(r, \theta, \varphi = 0, \omega) = u_z(r, \theta, \omega)\mathbf{e}_z + u_x(r, \theta, \omega)\mathbf{e}_x, \qquad (3)$$

where $u_x(r, \theta, \omega)$ and $u_z(r, \theta, \omega)$ are the projections of the velocity field vector into the X and Z axes, respectively, and $\mathbf{e}_x$, $\mathbf{e}_z$ are unit vectors directed along these axes. For the isoscalar dipole excitations, the functions $u_x(r, \theta, \omega)$ and $u_z(r, \theta, \omega)$ have the same form as for the isovector ones, see Ref. [25]. The difference is in the external field that is given by Eq. (1) for the isoscalar dipole excitations. So, we get

$$u_z(r, \theta, \omega) = Y_{00}(\theta, 0)u_{10}(r, \omega) -$$
$$- \sqrt{\frac{2}{5}} Y_{20}(\theta, 0)u_{12}(r, \omega), \qquad (4)$$

$$u_x(r, \theta, \omega) = \sqrt{\frac{3}{5}} Y_{21}(\theta, 0)u_{12}(r, \omega). \qquad (5)$$

Here, $Y_{lm}(\theta, \varphi)$ are spherical functions. The functions $u_{10}(r, \omega)$ and $u_{12}(r, \omega)$ describe the radial dependence
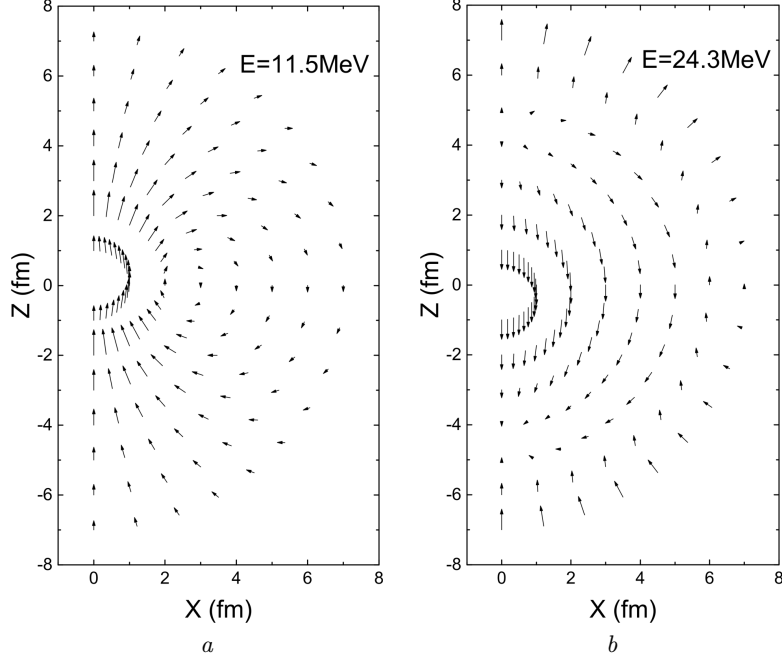
Fig. 2. Velocity fields in the XZ-plane related to the low- and high-energy isoscalar dipole resonances in a system of $A = 208$ nucleons. The velocity fields are calculated at energies of 11.5 MeV (*a*) and 24.3 MeV (*b*), which correspond to the energies of the low- and high-energy resonance peaks (the centroid energies), respectively, see Fig. 1

of the velocity field and are given by

$$u_{12}(r,\omega) = -i\sqrt{\frac{2}{3}}\pi \frac{1}{\rho_0} \frac{1}{r^2} \int d\varepsilon \int dl\, l \times$$

$$\times \sum_{N=-1}^{1} \left\{ -i \left[\delta\tilde{n}_N^+(r,\varepsilon,l,\omega) - \delta\tilde{n}_N^-(r,\varepsilon,l,\omega) \right] + \right.$$

$$\left. + \frac{N}{2} \frac{l}{p(r,\varepsilon,l)\, r} \left[\delta\tilde{n}_N^+(r,\varepsilon,l,\omega) + \delta\tilde{n}_N^-(r,\varepsilon,l,\omega) \right] \right\}, \quad (6)$$

$$u_{10}(r,\omega) = -i\sqrt{\frac{1}{3}}\pi \frac{1}{\rho_0} \frac{1}{r^2} \int d\varepsilon \int dl\, l \times$$

$$\times \sum_{N=-1}^{1} \left\{ i \left[\delta\tilde{n}_N^+(r,\varepsilon,l,\omega) - \delta\tilde{n}_N^-(r,\varepsilon,l,\omega) \right] + \right.$$

$$\left. + N \frac{l}{p(r,\varepsilon,l)\, r} \left[\delta\tilde{n}_N^+(r,\varepsilon,l,\omega) + \delta\tilde{n}_N^-(r,\varepsilon,l,\omega) \right] \right\}, \quad (7)$$

where ε is the particle energy, l is the magnitude of its angular momentum, $p(r,\varepsilon,l) = p_F \sqrt{1 - (l/p_F r)^2}$ is radial momentum, and the functions $\delta\tilde{n}_N^\pm(r,\varepsilon,l,\omega)$ are the solutions of the linearized Vlasov kinetic equation for a finite system with moving surface, see Appendix A.

3. Character of Isoscalar Dipole Velocity Fields

The numerical calculations of the dipole velocity field (3) were carried out for a Fermi system with the number of nucleons $A = 208$. In our calculations, we used the following standard values of nuclear parameters: $r_0 = 1.25$ fm, $\varepsilon_F = 30.94$ MeV, and $m = 1.04$ MeV $(10^{-22}s)^2/\text{fm}^2$. The parameter of the isoscalar dipole interaction strength is equal to $\kappa_1 = -7.5 \times 10^{-3}$ MeV/fm^2 and is determined by comparison with the giant monopole resonance data in nucleus ^{208}Pb within our kinetic model [15]. The corresponding value of the incompressibility modulus equals $K_A = 160$ MeV [22]. It should be noted that this parameter is smaller than in quantum approaches [11, 17, 20, 21].

In Fig. 1, the isoscalar dipole strength function $S(E)$ ($E = \hbar\omega$) is shown for a system withh $A = 208$ nucleons. This function is determined by the imaginary part of the isoscalar dipole response function calculated in Ref. [23], see Eq. (24). We can see that the isoscalar dipole strength function has a two-resonance structure. The centroid energies of the low- and the high-energy isoscalar dipole resonances equal 11.5
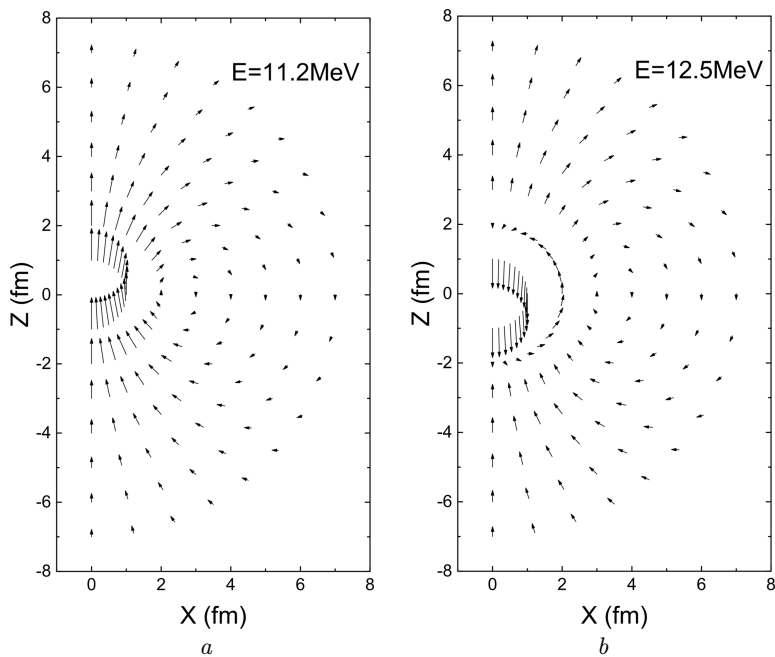
Fig. 3. Velocity fields for the low-energy isoscalar dipole resonance calculated at energies of 11.2 MeV (*a*) and 12.5 MeV (*b*) within the resonance width, see Fig. 1. Velocity field at the centroid energy equal to 11.5 MeV is shown in Fig. 2, *a*. The system contains $A = 208$ nucleons
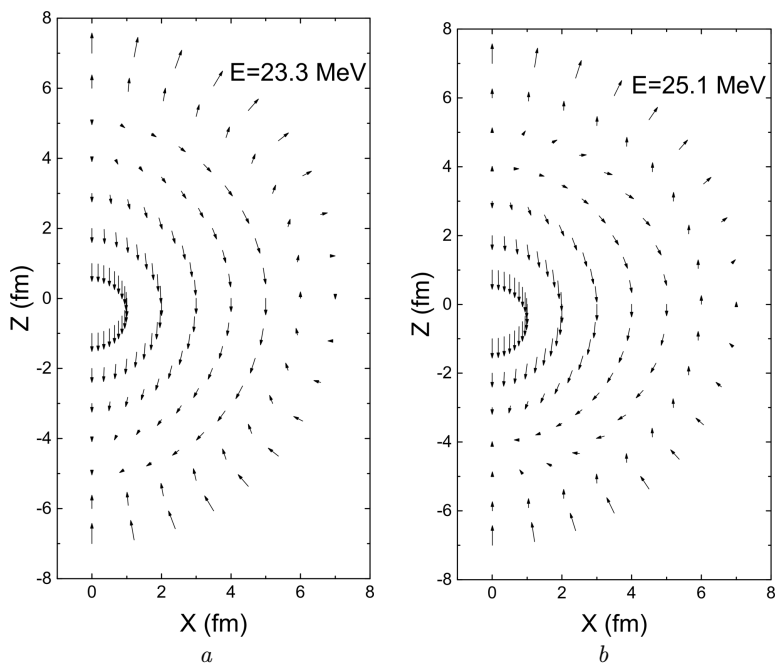
Fig. 4. Velocity fields for the high-energy isoscalar dipole resonance calculated at energies of 23.3 MeV (*a*) and 25.1 MeV (*b*) within the resonance width, see Fig. 1. Velocity field at the centroid energy equal to 24.3 MeV is shown in Fig. 2, *b*. The system contains $A = 208$ nucleons

and 24.3 MeV, respectively, in the agreement with experimental data for the isoscalar dipole resonances in ^{208}Pb nucleus [3, 4].

The results of numerical calculations of the velocity field (3) at centroid energies of 11.5 and 24.3 MeV corresponding to the low- and high-energy isoscalar dipole resonances (see Fig. 1) are shown in Fig. 2. The velocity field related to the low-energy resonance has a pure vortex character, see Fig. 2, *a*, while the velocity field for the high-energy resonance shows the compression character, see Fig. 2, *b*. The character of the velocity fields (vortex and compression) for the isoscalar dipole resonances, which is found in this paper in a semiclassical model, is in qualitative agreement with the previous results of relevant random-phase-approximation (RPA) calculations [11, 17, 20, 21]. To make a more detailed comparison , in particular, in the low-energy region, it is reasonable to study the dipole excitations associated with the toroidal operator [9, 19] in our semiclassical approach. However, this is left for the future work.

In Figs. 3 and 4, the evolution of the velocity field character depending on the excitation energy of the nucleus within the resonance width is shown. The velocity fields for the low-energy isoscalar dipole resonance are calculated at excitation energies of 11.2 and 12.5 MeV, see Figs. 3, *a* and 3, *b*. We can see that the velocity fields for the low-energy resonance keep the vortex character at the excitation energies within the resonance width. However, as the excitation energy increases, the velocity field for this resonance also has the compression, see Fig. 3, *b*. It is reasonable to assume that this effect displays the coupling between the low- and high-energy isoscalar dipole resonances, which was discussed in Ref. [17]. The velocity field evolution for the high-energy isoscalar dipole resonance is shown at excitation energies of 23.3 and 25.1 MeV, see Figs. 4, *a* and 4, *b*. This resonance preserves the compression character at the excitation energies within the resonance width, but the compression-expansion region of the velocity fields shifts inside the system, when changing the excitation energy.

4. Conclusions

The velocity fields related to the low- and high-energy isoscalar dipole resonances in heavy nuclei have been considered within the translation-invariant kinetic model of small oscillations of finite Fermi systems. It is found that the velocity field of the low-energy isoscalar dipole resonance at the centroid energy has an essentially vortex character. However, at increasing the excitation energy of a nucleus within the resonance width, this collective excitation can also involve a compression. This result verifies the coupling between the vortical and compression isoscalar dipole modes, which was found in Ref. [17]. Our study confirms the anisotropic ("squeezing") compression character of the high-energy isoscalar dipole resonance and discovers that the compression-expansion region of the velocity field shifts inside the nucleus with a change in the excitation energy within the resonance width.

As a final comment, we would like to add that the absence of the low-energy isoscalar dipole mode in the liquid drop model [26] gives a reason to assume that the dynamic deformation of the Fermi surface plays an important role in the formation of the low-energy resonance. To clarify this point, it is of interest to study the character of the momentum flux related to this resonance.

APPENDIX A
Fluctuations of the phase-space density for the isoscalar dipole excitations

In this appendix, we give the explicit expression for fluctuations of the phase-space distribution function related to collective isoscalar dipole excitations.

Solving the linearized Vlasov equation with boundary conditions at the moving surface, we can obtain an explicit expression for fluctuations of the phase-space particle distribution function. It can be written as [22]:

$$\delta \tilde{n}_N^{\pm}(r, \varepsilon, l, \omega) = \delta_{N,3}^{0\pm}(r, \varepsilon, l, \omega)[1 + \kappa_1 \, \tilde{R}_{13}^V(\omega)] +$$
$$+ \, \delta \tilde{n}_N^{s\pm}(r, \varepsilon, l, \omega). \tag{A.1}$$

The functions $\delta n_{N,k}^{0\pm}(r, \varepsilon, l, \omega)$ in Eq. (A.1) are the solutions of the Vlasov equation for a system of noninteracting nucleons confined by a fixed surface [22]:

$$\delta n_{N,k}^{0\pm}(r, \varepsilon, l, \omega) = -\beta \frac{\partial n_0(\varepsilon)}{\partial \varepsilon} \times$$
$$\times \sum_{n=-\infty}^{\infty} \omega_{nN}(\varepsilon, l) e^{\pm i \, [\omega_{nN}(\varepsilon, l)\tau(r, \varepsilon, l) + N\gamma(r, \varepsilon, l)]} \times$$
$$\times \frac{Q_{nN}^k(l)}{\omega - \omega_{nN}(\varepsilon, l) + i\eta}, \tag{A.2}$$

where $n_0(\varepsilon)$ is the equilibrium particle distribution function in the Thomas–Fermi approximation; $\omega_{nN}(\varepsilon, l) = n\frac{2\pi}{T(\varepsilon,l)} + N\frac{\Gamma(\varepsilon,l)}{T(\varepsilon,l)}$ are single-particle frequencies; and $T(\varepsilon, l)$, $\Gamma(\varepsilon, l)$ are the periods of the radial and "angular" particle motions. In Eq. (A.2), the classical limit for the radial matrix elements of the quantum-mechanical dipole operators $Q_{nN}^k(x)$ is given by

$$Q_{nN}^1(x) = (-1)^n R \frac{1}{s_{nN}^2(x)}, \tag{A.3}$$

$$Q_{nN}^3(x) = 3R^2 Q_{nN}^1(x) \left(1 + \frac{4}{3} N \frac{\sqrt{1-x^2}}{s_{nN}(x)} - \frac{2}{s_{nN}^2(x)} \right). \tag{A.4}$$

In Eqs. (A.3), (A.4) we use the dimensionless variables

$$s = \frac{\omega}{v_{\rm F}/R}, \quad s_{nN} = \frac{\omega_{nN}}{v_{\rm F}/R},$$

$$x = \sqrt{1 - (l/p_{\rm F}R)^2}, \quad s_{nN}(x) = \frac{n\pi + N\arcsin(x)}{x}.$$

The functions $\delta\tilde{n}_N^{s\pm}(r, \varepsilon, l, \omega)$ in Eq. (A.1) associated with the moving surface are given by [22]

$$\delta\tilde{n}_N^{s\pm}(r, \varepsilon, l, \omega) = \frac{\partial n^0(\varepsilon)}{\partial \varepsilon} \frac{e^{\pm i[\omega\tau(r,\varepsilon,l) + N\gamma(r,\varepsilon,l)]}}{\sin[\omega T(\varepsilon,l) + N\Gamma(\varepsilon,l)]} \times$$

$$\times p(R, \varepsilon, l)\omega\delta R_3(\omega). \tag{A.5}$$

Here $2\tau(r, \varepsilon, l)\big|_{r=R} = T(\varepsilon, l)$; $2\gamma(r, \varepsilon, l)\big|_{r=R} = \Gamma(\varepsilon, l)$ and $\delta R_3(\omega)$ is the variation of the equilibrium radius R of the system induced by the external field (1)

$$\delta R_3(\omega) = \beta \frac{R^4 \left(\chi_3^0 + \kappa_1 \rho_0 R^3 R_{11}^0(\omega) \right)}{-\chi_1 \left(1 - \kappa_1 R_{11}^0(\omega) \right) + \kappa_1 R^6 \left(\chi_1^0 + \rho_0 R \right)^2}, \tag{A.6}$$

where the parameter κ_1 describes the isoscalar dipole interaction strength. The functions $\chi_k^0(\omega)$ and $\chi_1(\omega)$ in Eq. (A.6) describe dynamic surface effects and are given by

$$\chi_k^0(s) = \frac{9A}{8\pi} \sum_{n=-\infty}^{+\infty} \sum_{N=\pm 1} \int_0^1 dx x^2 s_{nN}(x) \times$$

$$\times \frac{(-1)^n Q_{nN}^{(k)}(x)}{s + i\varepsilon - s_{nN}(x)} \quad (k = 1, 3), \tag{A.7}$$

$$\chi_1(s) = -\frac{9A}{4\pi} \varepsilon_{\rm F}(s + i\varepsilon) \sum_{n=-\infty}^{+\infty} \sum_{N=\pm 1} \int_0^1 dx x^2 \times$$

$$\times \frac{1}{s + i\varepsilon - s_{nN}(x)}, \tag{A.8}$$

where $\varepsilon_{\rm F}$ is the Fermi energy. The function $R_{11}^0(\omega)$ in Eq. (A.6) is the single-particle response function of the system confined by a fixed surface

$$R_{jk}^0(s) = \frac{9A}{16\pi} \frac{1}{\varepsilon_{\rm F}} \sum_{n=-\infty}^{+\infty} \sum_{N=\pm 1} \int_0^1 dx x^2 s_{nN}(x) \times$$

$$\times \frac{Q_{nN}^j(x) Q_{nN}^k(x)}{s + i\varepsilon - s_{nN}(x)}, \quad (j, k = 1, 3). \tag{A.9}$$

Finally, the function $\tilde{R}_{13}^V(\omega)$ in Eq. (A.1) is defined as

$$\tilde{R}_{13}^V(\omega) = \frac{R_s(\omega) + R_{13}^0(\omega)}{1 - \kappa_1 R_{11}^0(\omega)}, \tag{A.10}$$

where

$$R_s(\omega) = -\frac{1}{\beta} R^2 \delta R_3(\omega) \left[\chi_1^0(\omega) + \rho_0 R \right]. \tag{A.11}$$

1. H.L. Clark, Y.-W.Lui, D.H. Youngblood. Isoscalar giant dipole resonance in ^{90}Zr, ^{116}Sn, and ^{208}Pb. it Phys. Rev. C **63**, 031301 (2001).

2. D.H. Youngblood *et al.* Isoscalar $E0-E3$ strength in ^{116}Sn, ^{144}Sm, ^{154}Sm, and ^{208}Pb. *Phys. Rev. C* **69**, 034315 (2004).

3. M. Uchida, H. Sakaguchi, M. Itoh, M. Yosoi, T. Kawabata, H. Takeda, Y. Yasuda, T. Murakami, T. Ishikawa, T. Taki, N. Tsukahara, S. Terashima, U. Garg, M. Hedden, B. Kharraja, M. Koss, B.K. Nayak, S. Zhu, M. Fujiwara, H. Fujimura, K. Hara, E. Obayashi, H.P. Yoshida, H. Akimune, M.N. Harakeh, M. Volkerts,. Isoscalar giant dipole resonance in Pb-208 via inelastic alpha scattering at 400 MeV and nuclear incompressibility. *Phys. Lett. B* **557**, 12 (2003).

4. M. Uchida, H. Sakaguchi, M. Itoh, M. Yosoi, T. Kawabata, Y. Yasuda, H. Takeda, T. Murakami, S. Terashima, S. Kishi, U. Garg, P. Boutachkov, M. Hedden, B. Kharraja, M. Koss, B.K. Nayak, S. Zhu, M. Fujiwara, H. Fujimura, H. P. Yoshida, K. Hara, H. Akimune, M.N. Harakeh. Systematics of the bimodal isoscalar giant dipole resonance. *Phys. Rev. C* **69**, 051301(R). (2004).

5. N. Van Giai, H. Sagawa. Monopole and dipole compression modes in nuclei. *Nucl. Phys. A* **371**, 1 (1981).

6. G. Colo, N. Van Giai, P.F. Bortignon, M.R. Quaglia. On dipole compression modes in nuclei. *Phys. Lett. B* **485**, 362 (2000).

7. M.L. Gorelik, M.H. Urin. Properties of the isoscalar giant dipole resonance *Phys. Rev. C* **64**, 047301 (2001).

8. S. Shlomo, A.I. Sanzhur. Isoscalar giant dipole resonance and nuclear matter incompressibility coefficient. *Phys. Rev. C* **65**, 044310 (2002).

9. J. Kvasil, N. Lo Iudice, Ch. Stoyanov, P. Alexa. Compressional and toroidal dipole modes in nuclei. *J. Phys. G: Nucl. Part. Phys.* **29**, 753 (2003).

10. J. Piekarewicz. Relativistic approach to isoscalar giant resonances in ^{208}Pb. *Phys. Rev. C* **62**, 051304(R) (2000).

11. D. Vretenar, A. Wandelt, P. Ring. Isoscalar dipole mode in relativistic random phase approximation. *Phys. Lett. B* **487**, 334 (2000).

12. E.N. Balbutsev, I.N. Mikhailov. Dynamics of nuclear integral characteristics. *J. Phys. G* **14**, 545 (1988).

13. E.B. Balbutsev, I.V. Molodtsova, A.V. Unzhakova. Compressional and toroidal dipole excitations of atomic nuclei. *Europhys. Lett.* **26**, 499 (1994).

14. V.M. Kolomietz, S. Shlomo. Isoscalar compression modes within fluid dynamic approach. *Phys. Rev. C* **61**, 064302 (2000).

15. V.I. Abrosimov, A. Dellafiore, F. Matera. Kinetic-theory description of isoscalar dipole modes. Nucl. Phys. A **697**, 748 (2002).

16. M. Urban. Pygmy resonance and torus mode within Vlasov dynamics. *Phys. Rev. C* **85**, 034322 (2012).

17. D. Vretenar, N. Paar, P. Ring, T. Nikšić. Toroidal dipole resonances in the relativistic random phase approximation. *Phys. Rev. C* **65**, 021301(R) (2002).

18. V.I. Abrosimov, A. Dellafiore, F. Matera. *Int. Conf. on Collective Motion in Nuclei under Extreme Condition. Book of Abstracts. Paris* (2003), P. 54.

19. J. Kvasil, V.O. Nesterenko, W. Kleinig, P.G. Reinhard, P. Vesely. General treatment of vortical, toroidal, and compression modes. *Phys. Rev. C* **84**, 034303 (2011).

20. A. Repko, P.-G. Reinhard, V.O. Nesterenko, J. Kvasil. Toroidal nature of the low-energy $E1$ mode. *Phys. Rev. C* **87**, 024305 (2013).

21. P.-G. Reinhard, V.O. Nesterenko, A. Repko, J. Kvasil. Nuclear vorticity in isoscalar $E1$ modes: Skyrme-random-phase approximation analysis. *Phys. Rev. C* **89**, 024321 (2014).

22. V.I. Abrosimov, A. Dellafiore, F. Matera. Collective motion in finite Fermi systems within Vlasov dynamics. *Phys. Part. Nucl.* **36**, 699 (2005).

23. V.I. Abrosimov, O.I. Davydovska. Residual interaction effect on isoscalar dipole modes in heavy nuclei. *Ukr. J. Phys.* **61**, No. 7, 565 (2016).

24. I. Hamamoto, H. Sagawa, X.Z. Zhang. Displacement fields of excited states in stable and neutron drip-line nuclei. *Nucl. Phys. A* **648**, 203 (1999).

25. V.I. Abrosimov, O.I. Davydovska. Vortex motion of nucleons at isovector dipole excitations of nuclei. *Ukr. J. Phys.* **52**, No. 11, 1030 (2007).

26. A. Bohr, B.R. Mottelson. *Nuclear Structure, Vol. 2: Nuclear Deformations* (Benjamin, 1975).

В.І. Абросімов, О.І. Давидовська

ПРИРОДА ІЗОСКАЛЯРНИХ
ДИПОЛЬНИХ РЕЗОНАНСІВ У ВАЖКИХ ЯДРАХ

Р е з ю м е

Ізоскалярний дипольний ядерний відгук виявляє низько- та високоенергетичні резонанси. Природа ізоскалярних дипольних резонансів у важких сферичних ядрах вивчається за допомогою трансляційно-інваріантної кінетичної моделі малих коливань в скінченних фермі-системах. Розрахунки поля швидкостей для енергії центроїду показують суто вихровий характер низькоенергетичного ізоскалярного дипольного резонансу в сферичних ядрах і підтверджують анізотропний стискувальний характер високоенергетичного резонансу. Вивчено еволюцію поля швидкостей в залежності від енергії збудження ядра в межах ширини резонансу. Встановлено, що низькоенергетичний ізоскалярний дипольний резонанс зберігає вихровий характер, однак при збільшенні енергії це колективне збудження також включає стиснення. Високоенергетичний резонанс зберігає характер стиснення зі зміною енергії збудження в межах ширини резонансу, але області стиснення та розширення поля швидкостей зміщуються всередині ядра.